



## Topographically induced height errors in predicted atmospheric loading effects

T. van Dam,<sup>1</sup> Z. Altamimi,<sup>2</sup> X. Collilieux,<sup>2</sup> and J. Ray<sup>3</sup>

Received 23 July 2009; revised 27 January 2010; accepted 22 February 2010; published 29 July 2010.

[1] Atmospheric pressure variations are known to induce vertical displacements of the Earth's surface with magnitudes large enough to be detected by geodetic observations. Estimates of these loading effects are derived using global reanalysis fields of surface pressure as input. The input surface pressure has a minimum spatial sampling, which does not capture true surface pressure variations due to high topographic variability in some regions. In this paper, we investigate the effect that unmodeled topographic variability has on surface pressure estimates and subsequent estimates of vertical surface displacements. We find that the estimated height changes from the topographic surface pressure can be significant (2–4 mm) for sites in regions of high topographic variability. When we compare the estimated height changes to Global Positioning System residuals from the 2005 International Terrestrial Reference Frame Realization, we find that the heights derived from the topographic surface pressure, versus those from the normal surface pressure, perform better at reducing the scatter on the height coordinate time series.

**Citation:** van Dam, T., Z. Altamimi, X. Collilieux, and J. Ray (2010), Topographically induced height errors in predicted atmospheric loading effects, *J. Geophys. Res.*, 115, B07415, doi:10.1029/2009JB006810.

### 1. Introduction

[2] To interpret Global Positioning System (GPS) height coordinates in terms of surface stress, tectonic motions, post-glacial rebound, water storage changes, etc., the contribution to the heights by nuisance effects must be reduced or, if possible, eliminated. One such nuisance effect is the displacement of the Earth's surface that is driven by temporal variations in atmospheric surface pressure. A significant fraction of the scatter in GPS observations of crustal displacements is known to be caused by atmospheric surface mass loading [e.g., Petrov and Boy, 2004; Scherneck et al., 2003; van Dam and Herring, 1994; van Dam et al., 1997, 1994; Schuh et al., 2004; Zerbini et al., 2001]. The amplitude of the signal is highly variable over the surface of the Earth. It is largest at the middle to high latitudes, where synoptic pressure extrema are largest, and at inland locations where the inverted barometer effect of the ocean is minimized. Thus, we would like to have at our disposal reliable loading models that can be used to reduce the atmospheric loading contributions to the GPS coordinate observations.

[3] In many studies, global models of surface atmospheric pressure, such as those generated by the European Center for Medium Range Weather Forecasts (ECMWF) or the

National Center for Environmental Predictions (NCEP), are commonly used to estimate atmospherically driven displacements of the Earth's surface [see, e.g., van Dam and Wahr, 1987; van Dam and Herring, 1994; van Dam et al., 1994; Petrov and Boy, 2004]. These data sets provide estimates of surface pressure at temporal samplings down to 3 hours and spatial samplings down to 1.125 degrees (approximately 250 to 112.5 km at the equator).

[4] From a geodetic perspective, there are two potential issues with these fields: (1) Is the accuracy of the surface pressure fields at the resolution published sufficient for geodetic analyses? (2) Is the spatial resolution of the fields sufficient for geodetic analyses?

[5] With regards to the first question, a comparison of radial surface displacements predicted using NCEP reanalysis ( $2.5^\circ \times 2.5^\circ$ ) and ECMWF Operational ( $1.0^\circ \times 1.0^\circ$ ) surface pressure fields, demonstrates that differences over a single year can have a scatter as large as 1.25 mm over most of Antarctica. Over most other continental areas, the scatter is closer to 0.5 mm. This comparison is not optimal as we are comparing the radial surface displacements from a 1-degree pressure model with that from a 2.5 degree pressure model. Further, a comparison between the two data sets does not reveal inaccuracies that may be common to both data sets. Nonetheless, the differences between the surface pressure fields are below the scatter observed in most geodetic height time series.

[6] In addition, the meteorological community has long been aware that surface pressure values provided by these global analyses are somewhat inaccurate over land due to the input surface topography, which is not adequately represented in the models [Trenberth et al., 1987; Trenberth and

<sup>1</sup>Faculté des Sciences, de la Technologie et de la Communication, University of Luxembourg, Luxembourg, Luxembourg.

<sup>2</sup>Laboratoire de Recherche en Géodésie Institut Géographique National, Marne-La-Vallée, France.

<sup>3</sup>National Geodetic Survey, NOAA, Silver Spring, Maryland, USA.

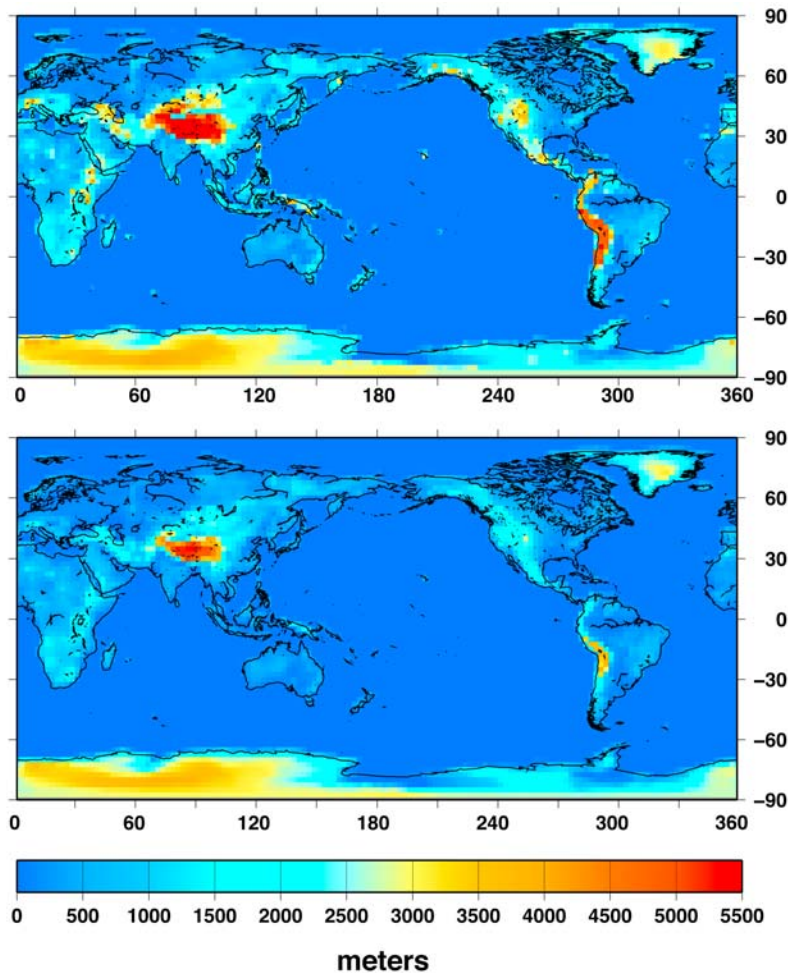


**Figure 1.** (top) Maximum topographic difference over areas of  $2.5^\circ$  in latitude and longitude using ETOPO5 topography at  $5'$  sampling. (bottom) Root-mean-square variability of elevation over areas of  $2.5^\circ$  in latitude and longitude.

*Smith, 2005*]. These errors are relatively small, geodetically speaking. A comparison of the NCEP  $2.5^\circ \times 2.5^\circ$  elevations with those from ETOPO5 [1988] indicates that less than 4% of the grid points exhibit differences greater than 200 m. The largest elevation differences occur in mountainous regions and always in isolation; i.e., the error is not coherent in space. A topographic error must be coherent over a large area (e.g., hundreds of kilometers) to produce a geodetically observable surface displacement. Thus, surface displacements from topographic errors at the given field resolution will be extremely small.

[7] The second issue, i.e., the spatial resolution of the meteorological fields in particular as compared to the higher spatial variability of the Earth's terrain, may be an issue for geodetic analyses. The problem can be stated like this: Surface pressure from the atmospheric circulation models are provided at a minimum spatial sampling. The surface pressure is assumed to have a constant value over this minimum grid size or spherical harmonic degree/order. If however, the topography in the grid cell exhibits large variability, then because the atmosphere is in hydrostatic equilibrium (pressure decreases/increases with increasing/decreasing elevation) the

surface pressure within the cell, in contrast to being constant over the area, will in reality vary significantly over the area of the grid cell. In other words, the current resolution of these surface pressure products (minimum grid size) is too large. Likewise, if surface pressure fields are recreated from the spherical harmonic representation of the field, the spherical harmonic degree cutoff is too low to capture the pressure effects due to real short-wavelength topography. Therefore, estimates of atmospheric loading effects for geodetic stations in regions of high topographic variability will be inaccurate.

[8] Figure 1 (top) shows the maximum change of the topography for grid units of dimension  $2.5^\circ \times 2.5^\circ$ . The value for each grid unit was determined by differencing the minimum and the maximum value in the grid using 5 minute topography data provided by ETOPO5. At many places on the continents, the maximum topographic difference within a grid unit can reach up to 2000 m. Larger changes are possible in regions where mountains exist.

[9] A change in geopotential height of 2000 m (geopotential height is approximately equal to geometric height in the troposphere) represents a change in pressure of about 200 hPa. If this load were coherent over an area of only 40 km, the

Earth's surface would displace downward by 4 mm. Thus, there is the potential for real short-wavelength changes in surface pressure due to topography, which are not captured by the coarse spatial sampling of the ECMWF or NCEP models, to contribute to observed surface displacements.

[10] Figure 1 (bottom) shows the scatter of the topography within each  $2.5^\circ \times 2.5^\circ$  grid unit. As the pressure for each grid cell is reported as constant, predicted pressure loading effects for grid cells with a large scatter in the topography will be in error.

[11] In this paper, we investigate the effect of high topographic variability on estimates of atmospheric loading induced surface displacements. We generate a high resolution surface pressure field using the NCEP reanalysis surface pressure fields ( $2.5^\circ \times 2.5^\circ$ ), ETOPO5 topography, and the fact that the atmosphere is in hydrostatic equilibrium. We then compare surface displacements predicted using the coarse and fine resolution surface pressure to estimate the magnitude of the topographic effect on geodetic station heights. We find that estimated height changes can reach 3 mm over very short periods. However, the scatter of the height differences, over the 6 year period investigated, is usually less than 1.5 mm.

[12] We then compare the estimated height changes from the two surface pressure models with GPS height residuals derived from the ITRF2005 combination [Altamimi *et al.*, 2007]. We find that heights from the topographic pressure model are significantly more effective at reducing the scatter on the geodetic height residuals than heights derived from the normal NCEP surface pressure data set: the topographic model reduces the scatter on 74% of the time series whereas the normal model only reduces the scatter on 48%. We also find that the topographic model is not perfect, and that there are some sites where the scatter on the heights increases. This is most likely due to errors in the original surface pressure model, the loading model, and/or errors in the GPS height coordinate observations.

## 2. Topographic Surface Pressure Data Sets

[13] To estimate the effects of unmodeled topographic surface pressure variations on the radial crustal displacement, we compare the predicted surface displacements derived using two surface pressure grids, both of which were derived from the NCEP Reanalysis (NECPR) surface pressure field ( $2.5^\circ \times 2.5^\circ$  latitude-longitude grid) [Kalnay *et al.*, 1996]. The first pressure field is essentially the NCEP surface pressure at finer spatial sampling,  $0.125^\circ \times 0.125^\circ$  spacing versus  $2.5^\circ \times 2.5^\circ$ . The second modeled pressure field, uses  $0.125^\circ \times 0.125^\circ$  global topography and the assumption that the atmosphere is in hydrostatic equilibrium to predict global surface pressure at  $0.125^\circ \times 0.125^\circ$  spacing.

[14] In the first model, NCEPR<sub>FINE</sub>, every  $0.125^\circ$  subcell that lies within an original  $2.5^\circ$  NECPR cell is first determined to be land or ocean using a corresponding  $0.125^\circ$  land/ocean mask. If the  $0.125^\circ$  subcell is land, it is assigned the elevation and pressure of the original  $2.5^\circ$  cell. If it is ocean, it is assigned an elevation of zero, and a pressure,  $p_{\text{ocean}}$ , which is determined by calculating the net change in pressure over the entire ocean area for that epoch, i.e.,

$$p_{\text{ocean}} = \frac{\int_s \Delta p dS}{A}, \quad (1)$$

where  $\Delta p$  is the change in pressure in every original  $0.125^\circ$  ocean grid cell,  $A$  is the surface area of the oceans and the integral is performed over the ocean surface.

[15] For the second surface pressure model, we determine the pressure at the  $0.125^\circ \times 0.125^\circ$  by using the barometric height formula [Zdunkowski and Bott, 2004]:

$$p(z) = p_0 \left( \frac{T_0 - \Gamma z}{T_0} \right)^{\frac{g}{R\Gamma}} \quad (2)$$

[16] In equation (2),  $T_0$  and  $p_0$  are the temperature and pressure at the reference level, the elevation of the original NCEPR  $2.5^\circ \times 2.5^\circ$  grid units.  $T_0$  and  $p_0$  are extracted from the original  $2.5^\circ \times 2.5^\circ$  NCEPR pressure fields. Also,  $g = 9.80665 \text{ m/s}^2$  is the acceleration due to gravity (which is constant if measured in terms of geopotential height),  $R = 287.04 \text{ J/(kg}^\circ\text{K)}$  is the gas constant,  $\Gamma = 0.006499^\circ\text{K/m}$  is the lapse rate of the temperature, and  $z$  is the geopotential height difference. The geopotential heights,  $z$ , represent the difference between the NCEPR  $2.5^\circ \times 2.5^\circ$  surface elevations and the elevations at every  $0.125^\circ \times 0.125^\circ$  determined from ETOPO5. The geometric elevations are converted to geopotential using equation (A1).

[17] We compare displacements computed using the NCEPR<sub>FINE</sub> estimated pressure field with those computed using NCEPR<sub>TOPO</sub> because we are only interested in the effects of topographic pressure differences on the displacements. If we had compared deformations computed using the NECPR<sub>TOPO</sub> with those computed using the original  $2.5^\circ$  NCEPR data set, we would be unable to interpret the results at coastal sites because any observed differences in the displacements would depend not only on the topographic pressure assumption but would also depend on the fact that we would be using a different resolution for our ocean mask.

[18] We arbitrarily use the 1800 hour record of the 6-hourly NCEPR surface pressure data for the 6 year period, 2000–2005, to generate the two pressure data sets, NCEPR<sub>FINE</sub> and NCEPR<sub>TOPO</sub>.

[19] In Figure 2, we show the RMS of the difference between NCEPR<sub>FINE</sub> and NCEPR<sub>TOPO</sub> pressure for each  $0.125^\circ$  from the entire 6 years of data. We observe that at most points over the continents, the RMS is well below 8 hPa. Over mountainous regions, the RMS of the pressure difference can reach 27 hPa. Note also, that the RMS can be between 4 and 8 hPa over many regions of the Antarctic continent. The results presented here for Antarctica, may be inaccurate as the lapse rate used in these calculations ( $\Gamma$  in equations (2) and (3)) may be at least 30% lower than the actual lapse rate over Antarctica [Radok *et al.*, 1996].

[20] We also compare the pressure differences at 285 specific geodetic locations for the 6 year period. The sites were chosen because these are locations where permanent International GNSS (Global Navigation Satellite System) Service (IGS) Global Positioning Systems (GPS) receivers are operating and these are sites used in the determination of ITRF2005 [Altamimi *et al.*, 2007]. For these stations (not shown), the RMS of the pressure difference (NCEPR<sub>FINE</sub> – NCEPR<sub>TOPO</sub>) is always less than 14 hPa. Maximum pressure differences on any given day at most sites are usually less than 15 hPa, however maximum differences of up to 50 hPa are observed at a few stations.

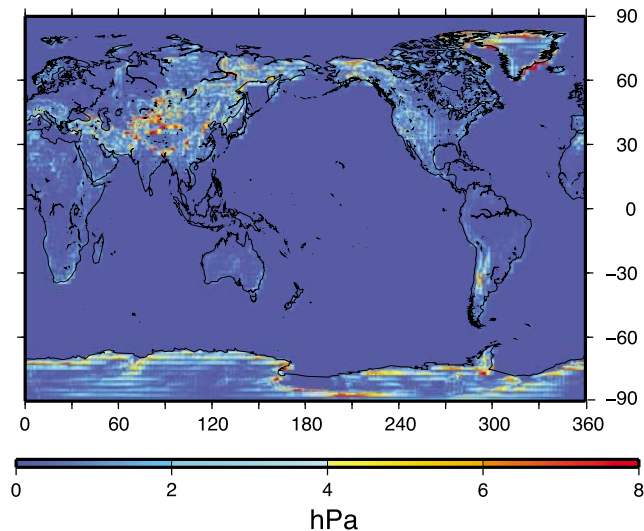


**Figure 2.** Root-mean-square variability of the difference between the control and topographic pressure grid over areas of  $.125^\circ$  in latitude and longitude.

[21] Time series of the local pressure difference ((NCEPR<sub>FINE</sub>) – (NCEPR<sub>TOPO</sub>)) for two stations are shown in Figure 3. The results for pol2, Bishkek, Kyrgyzstan, a site where the topography has one of the largest effects, are shown in black. In red, we show pressure differences from a more typical site graz, Graz, Austria. At pol2 we see that day-to-day differences of 10 hPa are common and that changes of 20–40 hPa can occur as well. At graz, day-to-day differences are much smaller, usually less than 2 hPa. The RMS of the pressure difference is 1.3 and 13.8 hPa for graz and pol2, respectively.

[22] In addition to the differences in the predicted day-to-day pressure from the two data sets, an annual signal is also observed in the time series shown in Figure 3. This observation is significant because understanding the cause of annual signals in GPS height coordinate time series has been a goal for more than a decade. For example, *Blewitt et al.* [2001] and *Wu et al.* [2003] among others, have used observed annual variations in GPS coordinates to invert for global-scale, seasonal variations in water storage. Others have found that there exists only a modest correlation between the annual signal in GPS heights and GRACE observations of the water storage signal [*van Dam et al.*, 2007; *Tregoning et al.*, 2009], presumably due to systematic errors in GPS hardware and data processing techniques.

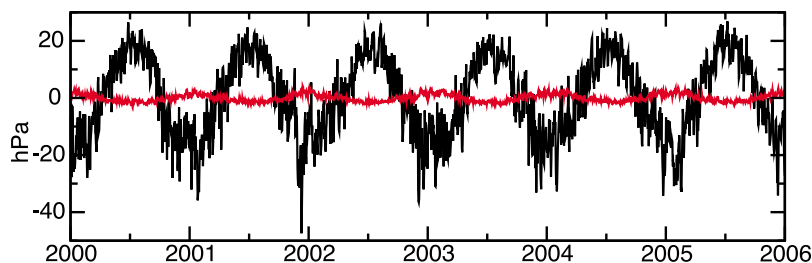


**Figure 3.** Difference between local NCEPR<sub>FINE</sub> and NCEPR<sub>TOPO</sub> pressure for pol2, Bishkek, Kyrgyzstan, in black, and graz, Graz, Austria in red.

[23] The annual signal may seem surprising given that what is shown in Figure 3 is the *difference* in pressure between the surface pressure at the elevation of the  $2.5^\circ$  grid cell and the pressure at the elevation of the station. The difference in elevation between the NCEPR geopotential height and the height of pol2 is 2100 m. For graz, the difference is only 350 m. One might expect that the surface pressure at points in the same vicinity (independent of altitude) would have the same annual signal, and thus, the difference in the pressure at the two points should not have an annual dependence. In fact, the annual signal at the different elevations has the same phase but a different amplitude. The difference in amplitude comes from the fact that the pressure at elevation,  $p'$ , is equal to the pressure at the reference elevation,  $p_0$  scaled by the effect of the lapse rate (Appendix B).

[24] In Figure 4 (top) we plot the RMS and in Figure 4 (bottom) we plot the maximum of the difference between the NCEPR<sub>FINE</sub> and NCEPR<sub>TOPO</sub> model pressures for all the stations used in this study. As expected, the RMS and maximum differences are largest for sites located in regions where the topography is highly variable over short distances (compare Figure 4 with Figure 1).

### 3. Modeling Surface Displacements

[25] The modeled pressure fields derived in section 2 are convolved with *Farrell's* [1972] elastic loading Green's functions to estimate the effects of the unmodeled topographic pressure changes on surface displacements.

[26] The vertical displacement at a point on the Earth's surface,  $du(\theta, \phi)$  (colatitude  $\theta$  and longitude  $\phi$ ), induced by the difference in surface pressure variations over a global grid  $\Delta P_{i,j} = \text{NCEPR}_{\text{TOPO}(i,j)} - \text{NCEPR}_{\text{FINE}(i,j)}$ , where each  $i, j$  represents a unique latitude and longitude is equal to

$$du(\theta, \phi) = \sum_{i=1}^{nlon} \sum_{j=1}^{nlat} \Delta P_{i,j} G_{i,j}^u A_{i,j} \quad (3)$$

where  $G_{i,j}^u$  is the radial Green's function [*Farrell*, 1972] that is a function of the angular distance between the load and the point on the Earth where the effect of the load is being determined, the limits  $nlon$  and  $nlat$  represent the number of grid unit increments in longitude and latitude, respectively, and  $A_{i,j}$  is the area of the grid unit.

[27] The loading effects are calculated using an Earth model in which the oceans respond as a modified inverted barometer [*van Dam and Wahr*, 1987] to pressure loading. We use a  $0.125^\circ$  resolution land-ocean mask to determine

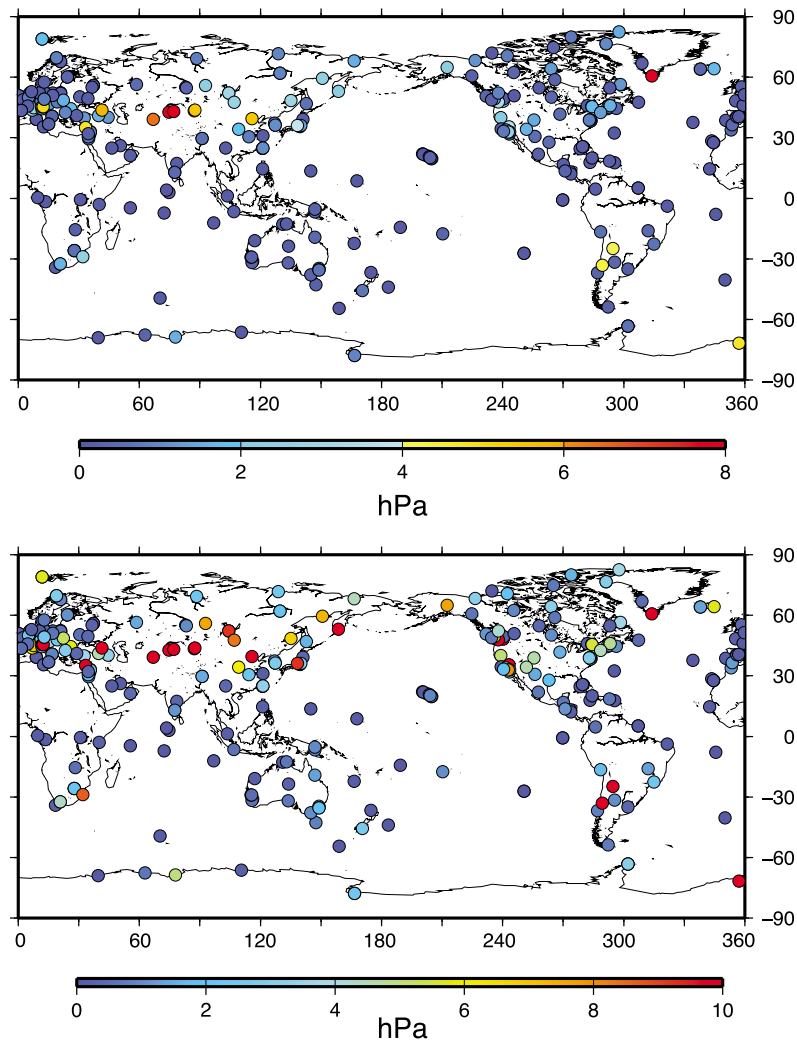


**Figure 4.** Location of sites used in determining the effect of topographic pressure effects. (top) The RMS of the pressure difference ( $\text{NCEPR}_{\text{FINE}} - \text{NCEPR}_{\text{TOPO}}$ ) at each station. (bottom) The maximum difference in pressure ( $\text{NCEPR}_{\text{FINE}} - \text{NCEPR}_{\text{TOPO}}$ ) for each station over the 6 year period investigated.

the net pressure changes over the oceans for each epoch as mentioned in section 2.

[28] Figure 5 (top) shows the RMS and Figure 5 (bottom) shows the maximum change in the height coordinate predicted for all sites over the 6 year period. Considering all the stations, the scatter in the height differences has a mean of less than 0.2 mm, with larger scatters being associated with sites in regions of high topographic variability. Maximum height coordinate differences can be as large as 5 mm.

[29] In Figure 6, we focus again on the stations po12 and graz. graz in red shows very small day-to-day variations ( $\text{RMS} < 0.2$  mm) over the time period investigated. po12, on the other hand, displays somewhat larger short period variations, e.g., 2–3 mm height differences are common. In addition, both sites show an annual signal in the height differences. For po12, the annual amplitude has a magnitude of 1.8 mm, whereas at graz the amplitude is only 0.3 mm.

[30] The percent difference,

$$\% \text{DIFF} = \frac{2 \times |\text{NCEPR}_{\text{FINE}} - \text{NCEPR}_{\text{TOPO}}|}{\text{NCEPR}_{\text{FINE}} + \text{NCEPR}_{\text{TOPO}}} \times 100,$$

between the heights determined using either  $\text{NCEPR}_{\text{TOPO}}$  or  $\text{NCEPR}_{\text{FINE}}$  provides some indication of how the heights from the two models compare. If  $\% \text{DIFF} = 0$ , then the models give the same result.

[31] In Figure 7 we show  $\% \text{DIFF}$  (blue dots), as well as the modeled height coordinate effects ( $\text{NCEPR}_{\text{FINE}}$  in black and  $\text{NCEPR}_{\text{TOPO}}$  in red) for the stations graz and po12 for each day of the 6 year comparison. The results at graz indicate that the heights from  $\text{NCEPR}_{\text{FINE}}$  differ from those from  $\text{NCEPR}_{\text{TOPO}}$  by 3% on average with a RMS of 40%. At po12, the values differ by  $-3\%$  on average but the RMS of  $\% \text{DIFF}$  in this case is 90%.

[32] In Figure 8, we plot the RMS of the  $\% \text{DIFF}$  for each site used in the study. At most sites, the  $\% \text{DIFF}$  is less than 40%, indicating relatively good agreement between the two models, such as we observed at graz. Approximately 55% of the stations have scatter in  $\% \text{DIFF}$  larger than 60%, which would indicate less agreement between the models.

[33] The results presented in this section demonstrate that the effect of topographic variations in surface pressure on modeled estimates of height changes can be substantially

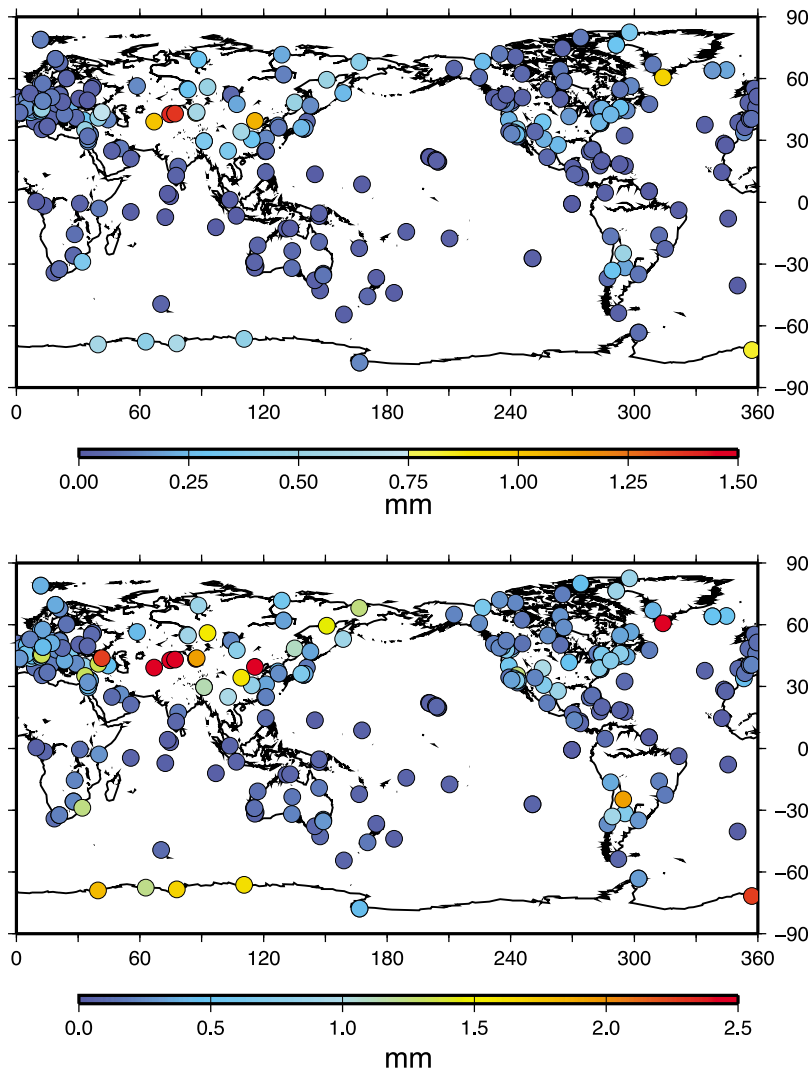


**Figure 5.** (top) The RMS of the predicted vertical surface displacement at a particular station due to the difference in the  $\text{NCEPR}_{\text{FINE}}$  and  $\text{NCEPR}_{\text{TOPO}}$ . (bottom) The maximum difference in height due to the different input pressures.

different than those heights modeled using the traditional surface pressure. The difference between the pressure models is largest for sites in regions of high topographic variability. In section 4, we compare observed GPS height residuals with loading predictions determined using the  $\text{NCEPR}_{\text{FINE}}$  and  $\text{NCEPR}_{\text{TOPO}}$  atmospheric pressure models to determine if the differences in the pressure models can have an observed effect.

#### 4. Comparison With Geodetic Observations

[34] As shown above, modeled atmospheric loading displacements can differ depending on whether the short scale topography is considered in the surface pressure input. In this section we compare observed GPS station height coordinate changes with height changes predicted using the two different pressure data sets,  $\text{NCEPR}_{\text{FINE}}$  and  $\text{NCEPR}_{\text{TOPO}}$ .

[35] The GPS time series used here are the nonlinear residuals generated in the ITRF2005 combination [Altamimi et al., 2007] from the weekly combined global frames pro-

duced by the IGS [Ferland, 2004]. In the ITRF2005 combination, each weekly IGS frame has been aligned to a self-consistent secular reference by applying a seven-parameter Helmert transformation relative to the long-term stacking. The full variance-covariance matrix for each IGS weekly frame has been used. Strictly linear site motions have been assumed including sites where discrete discontinuities have been introduced, usually based on empirical evidence but often corresponding to equipment changes.

[36] To compare our predicted height changes with the ITRF2005 residuals, daily height estimates derived using each of the two modeled input pressure data sets were averaged into weekly values centered on the GPS week to correspond to the sampling of the GPS height residuals. The temporal overlap between the atmospheric pressure data used in the analysis above and the ITRF residuals is about 300 of the full 312 weeks. We restrict the comparison to height coordinate time series with more than 100 weekly observations to improve the reliability of the statistical results. This leaves us with height coordinate time series

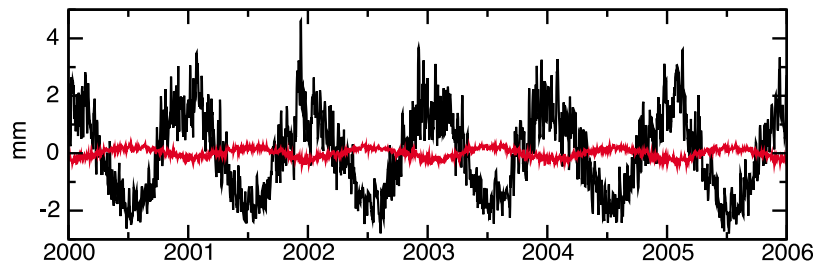


**Figure 6.** NCEPR<sub>FINE</sub> and NCEPR<sub>TOPO</sub> height differences for po12, Bishkek, Kyrgyzstan, in black, and graz, Graz, Austria in red.

from 246 stations to compare with the predicted height changes from the NCEPR<sub>FINE</sub> and NCEPR<sub>TOPO</sub> surface pressure.

[37] Of the 246 GPS height coordinate time series that we investigated, the RMS of the GPS residuals was decreased (improved) on 117 sites (48%) by removing the radial surface displacements predicted using NCEPR<sub>FINE</sub> whereas the RMS on 181 of the height coordinate time series (74%) decreased when the NCEPR<sub>TOPO</sub> loading effects were removed from the GPS heights.

[38] Figure 9 shows the RMS change at each site as a function of the variability of the regional topography (0.125° topography within 300 km of the site). The RMS of the data corrected using NCEPR<sub>FINE</sub> are represented by the black crosses; the data corrected using NCEPR<sub>TOPO</sub>, by the red crosses. Crosses above zero indicate sites whose height coordinate time series have been improved using the model;

crosses below are sites where the data have been degraded. It is clear from Figure 9 that there are more red crosses above the zero line and more black crosses below, indicating that the topographic surface pressure model represents an improvement over our model that does not consider topography. Unexpectedly, there appears to be no correlation with the regional topography. The NCEPR<sub>TOPO</sub> model appears to outperform NCEPR<sub>FINE</sub> at almost all sites analyzed.

[39] Of the 65 sites where applying NCEPR<sub>TOPO</sub> loading effects increased the scatter, the RMS on 62 sites was increased even more by applying the NCEPR<sub>FINE</sub> loading correction. Thus, when you mismodel the atmospheric loading effects you introduce an even larger error into your GPS residuals using NCEPR<sub>FINE</sub> rather than NCEPR<sub>TOPO</sub>.

[40] There are 52 GPS sites where NCEPR<sub>FINE</sub> does better than NCEPR<sub>TOPO</sub> at reducing the scatter on the height coordinates. However, there is no obvious explanation as

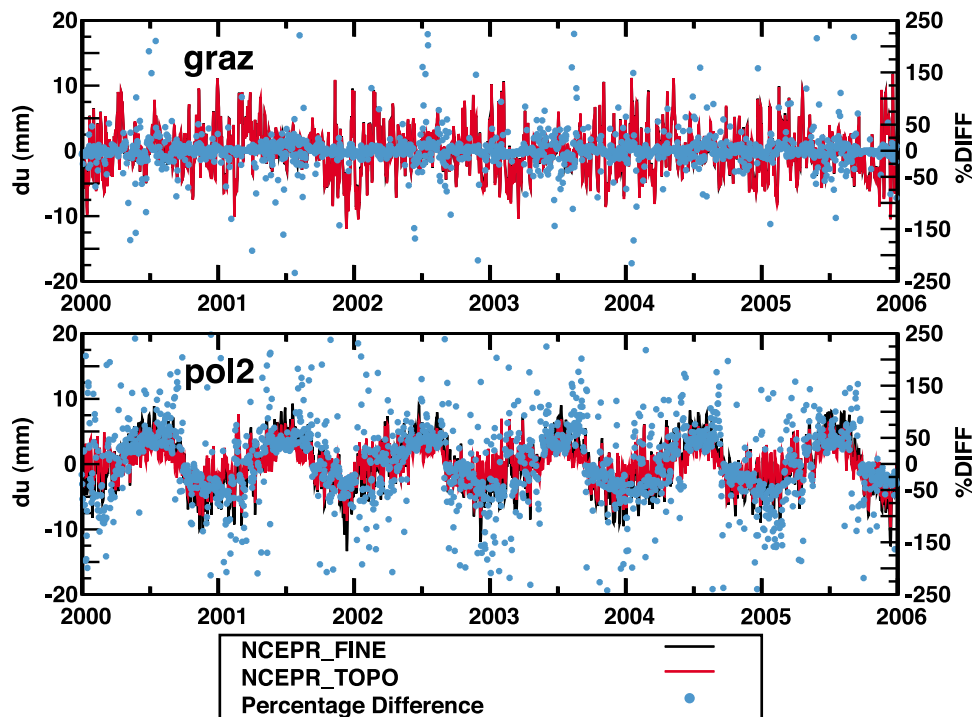


**Figure 7.** The percentage difference in the RMS of GPS heights before and after correcting for atmospheric loading using NCEPR<sub>FINE</sub> as opposed to NCEPR<sub>TOPO</sub>. The black line is the correction from NCEPR<sub>FINE</sub> (left hand y axis); the red line is the correction from NCEPR<sub>TOPO</sub> (left hand y axis). Blue dots represent the percentage difference (right hand y axis).

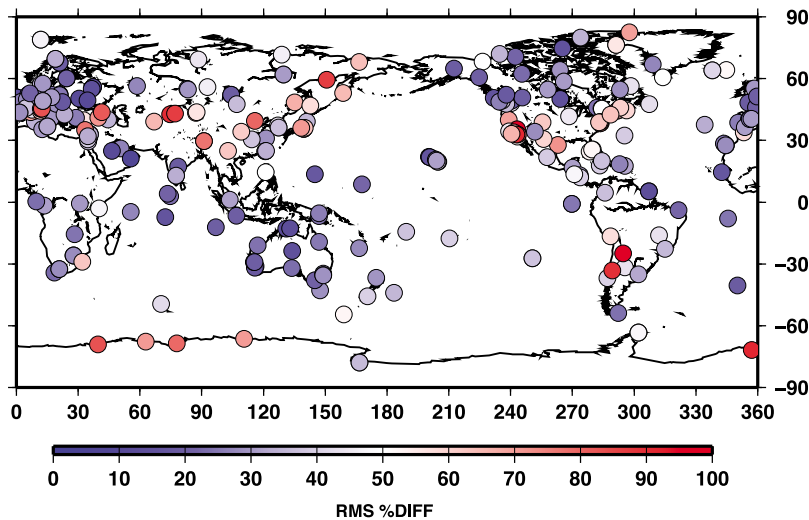


**Figure 8.** The RMS of the %DIFF calculated for sites analyzed in this paper.

to why the NCEPR<sub>FINE</sub> model does better at these sites. There appears to be no correlation with the scatter of the regional topography for these sites.

[41] In summary, this comparison of GPS observed height coordinate time series with the NCEPR<sub>FINE</sub> and NCEPR<sub>TOPO</sub> surface pressure models indicates that there is a clear tendency for atmospheric loading effects determined using a topographically dependent surface pressure to reduce the scatter more than a pressure model without topography considered.

[42] There are cases where neither loading model reduces the scatter on the GPS height coordinates. This lack of improvement could be due to a number of causes including (1) errors in the original NCEPR surface pressure from which the NCEPR<sub>FINE</sub> and NCEPR<sub>TOPO</sub> models are derived, (2) errors in the ocean mask, and/or (3) errors in the lapse rate that was taken as constant here but which can vary depending on radiation, convection, condensation, and whether the air is moist or dry. In addition, GPS height coordinates are known to contain (1) errors, which are unrelated to surface

displacements, and (2) other environmental loading signals, e.g., water storage variability, which is much larger than the atmospheric loading studied here, and nontidal ocean loading, which is much smaller. Thus, for sites where applying atmospheric loading corrections does not improve the scatter, each site must be regarded individually to determine if the atmospheric model is in error or if there is some other signal in the GPS heights causing the problem.

### 5. Conclusions

[43] Atmospheric loading in geodetic time series is a zero sum effect. If one is interested in establishing trends for interpreting tectonics, postglacial rebound, or water mass changes due to global warming, the atmospheric loading effects average to zero over time. However, the error bar on a trend derived from any data set is proportional to the scatter on the data. One way to reduce the error bar is with long observation times. Another method is to reduce the noise on the data. In this paper, we investigate a method for improving

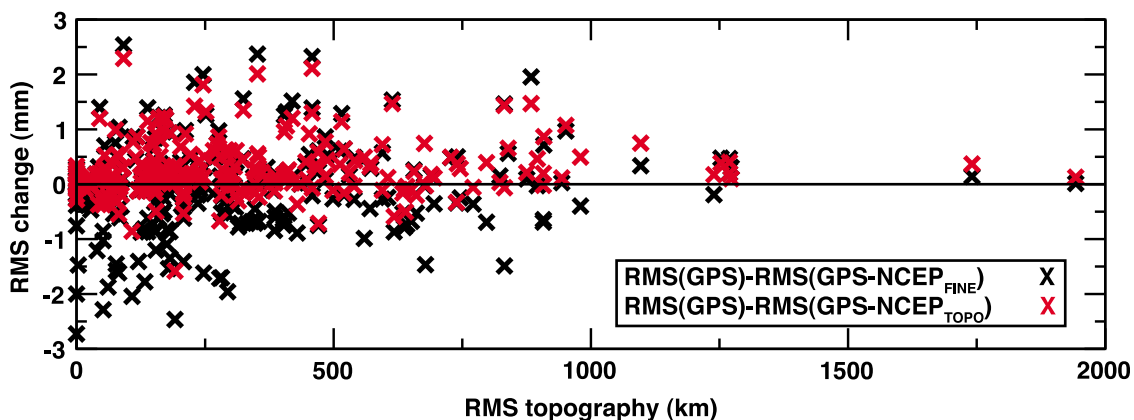


**Figure 9.** The RMS change on the GPS height time series using heights predicted from the NCEPR<sub>FINE</sub> and NCEPR<sub>TOPO</sub> data sets as a function of the RMS of the regional topography (0.125° topography within 300 km of the site). RMS change for NCEPR<sub>FINE</sub>, black crosses, and RMS change for NCEPR<sub>TOPO</sub>, red crosses.

our ability to remove atmospheric loading signals from GPS height coordinate time series.

[44] In particular, we have investigated the effect of unmodeled topographic variations in surface pressure on estimates of radial surface displacements at geodetic sites. We estimated surface height changes from two modeled surface pressure fields, both of which were derived from the 2.5° NCEP reanalysis surface pressure. The first data set, NCEPR<sub>FINE</sub> is a resampling of the original NCEP surface pressure at 2.5° × 2.5° resolution to 0.125° × 0.125°. The second data set, NCEPR<sub>TOPO</sub>, also with a 0.125° sampling, accounts for the change in pressure associated with changes in surface topography within the original 2.5° grid cell. In both new modeled fields, a 0.125° ocean mask was applied.

[45] We find that the difference between the heights derived from NCEPR<sub>FINE</sub> and NCEPR<sub>TOPO</sub> are in general quite small on a day-to-day basis. However, short-period height differences of 2 mm are common at stations in regions of high topographic variability. We also find, that the annual signal in the heights estimated from the two different data sets can be significant. (An analysis of the annual signal with respect to the GPS heights is left as further research as annual signals in GPS height coordinates themselves can be somewhat inconsistent even with respect to the larger magnitude annual water storage signal.)

[46] When we compare the predicted height changes to observed GPS height coordinate residuals, we find that NCEPR<sub>TOPO</sub> derived heights do significantly better at reducing the scatter on the observed GPS height coordinates rather than the heights estimated using NCEPR<sub>FINE</sub>. However, neither model improves the scatter on some height coordinate time series. This may be due to errors in the model, errors in the GPS height coordinates, and/or the existence of larger amplitude environmental signals in the data.

## Appendix A: Geometric to Geopotential Heights

[47] We begin by using the relationship between geometric heights,  $h$ , and geopotential heights,  $z$ , provided by M. J. Mahoney (A discussion of various measures of altitude, unpublished manuscript, 2001, available at <http://mtp.jpl.nasa.gov/notes/altitude/altitude.html>) for the WGS-84 ellipsoid:

$$z(h, \phi) = \frac{\gamma_s(\phi) R(\phi) \times h}{\gamma_{45} R(\phi) + h} \quad (\text{A1})$$

where  $\gamma_{45} = 9.80665 \text{ m/s}^2$ , is value of normal gravity at 45° latitude (halfway between the minimum and maximum value at the equator and poles, respectively).

[48] The radius  $R(\phi)$ ,

$$R(\phi) = \left( \frac{\cos^2(\phi)}{a^2} + \frac{\sin^2(\phi)}{b^2} \right)^{-1/2} \quad (\text{A2})$$

is the radius of the WGS84 ellipsoid at latitude  $\phi$ .  $a$  is the semimajor axis of the WGS-84 ellipsoid and  $b$  is the semi-minor axis. ( $R(\phi)$  introduced here, is not to be confused with the gas constant,  $R$ , introduced in section 2):

$$\gamma_s(\phi) = \gamma_e \frac{1 + k_S \sin^2(\phi)^2}{\sqrt{1 - e^2 \sin^2(\phi)^2}} \quad (\text{A3})$$

is the value of gravity on the ellipsoid defined by the eccentricity  $e = 0.0066943800229$ , Somigliana's constant,  $k_S = 1.931853 \times 10^{-3}$ , and  $\gamma_e = 9.7803267714$  is the value of gravity at the equator [Heiskanen and Moritz, 1967].

[49] The WGS-84 ellipsoid is itself defined by the flattening  $f = (a - b)/a = 1/298.257223560$  where  $a = 6378137.0$  and  $b = 6356752.3$ .

## Appendix B: Annual Signal in the Pressure Difference

[50] The difference between the pressure at the two elevations is

$$\Delta p = p_0 - p' = p_0 - p \left( \frac{T'}{T_0} \right)^{g/RT}$$

where  $p_0$  is the NCEPR surface pressure,  $T_0$  is the NCEPR temperature, both in the 2.5° grid cell, and  $p'$  and  $T'$  are the computed temperature and pressure, respectively, at the elevation of the 0.125° subgrid containing the station. Both temperature and pressure variables have an annual signal.  $T_0$  and  $T'$  at the two points differ only by a constant so that the annual signals in the fraction,  $T'/T_0$ , cancel out. The annual in  $p'$  then has the same phase as the annual in  $p_0$  but has a different amplitude,  $(T'/T_0)^{g/RT}$ . When  $\Delta p$  is calculated, the amplitudes of the annual signals in the pressure at the different elevations do not cancel out.

## References

- Altamimi, Z., X. Collilieux, J. Legrand, B. Garayt, and C. Boucher (2007), ITRF2005: A new release of the International Terrestrial Reference Frame based on time series of station positions and Earth orientation parameters, *J. Geophys. Res.*, *112*, B09401, doi:10.1029/2007JB004949.
- Blewitt, G., D. Lavallee, P. Clarke, and K. Nurudinov (2001), A new global model of Earth deformation: Seasonal cycle detected, *Science*, *294*, 2342–2345, doi:10.1126/science.1065328.
- ETOPO5 (1988), Data Announcement 88-MGG-02, Digital relief of the surface of the Earth, Natl. Geophys. Data Cent., Boulder, Colo.
- Farrell, W. E. (1972), Deformation of the Earth by surface loads, *Rev. Geophys. Space Phys.*, *10*(3), 761–797, doi:10.1029/RG010i003p0761.
- Ferland, R. (2004), Reference frame working group technical report, in *IGS 2001–2002 Technical Reports*, edited by K. Gowey, R. Neilan, and A. Moore, *JPL Publ.*, *04-017*, 25–33. (Available electronically at [igs.jpl.nasa.gov/overview/pubs.html](http://igs.jpl.nasa.gov/overview/pubs.html))
- Heiskanen, W., and H. Moritz (1967), *Physical Geodesy*, 364 pp., W.H. Freeman, San Francisco.
- Kalnay, E., et al. (1996), The NCEP/NCAR 40-Year Reanalysis Project, *Bull. Am. Meteorol. Soc.*, *77*(3), 437–471, doi:10.1175/1520-0477(1996)077<0437:TNYRP>2.0.CO;2.
- Petrov, L., and J. P. Boy (2004), Study of the atmospheric pressure loading signal in very long baseline interferometry observations, *J. Geophys. Res.*, *109*, B03405, doi:10.1029/2003JB002500.
- Radok, U., I. Allison, and G. Wendler (1996), Atmospheric surface pressure over the interior of Antarctica, *Antarct. Sci.*, *8*, 209–217, doi:10.1017/S0954102096000284.
- Scherneck, H.-G., J. M. Johansson, H. Koivula, and T. van Dam (2003), T. and J.L. Davis, Vertical crustal motion observed in the BIFROST project, *J. Geodyn.*, *35*, 425–441, doi:10.1016/S0264-3707(03)00005-X.
- Schuh, H., G. Easterman, J.-F. Cretaux, M. Berge-Nguyen, and T. van Dam (2004), Investigation of hydrological and atmospheric loading by space geodetic techniques, in *International Workshop on Satellite Altimetry for Geodesy, Geophysics and Oceanography, IAG Symp.*, vol. 126, edited by C. Hwang, C.-K. Shum, and J. C. Li, pp. 123–132, Springer-Verlag, Berlin.
- Tregoning, P., C. Watson, G. Ramillien, H. McQueen, and J. Zhang (2009), Detecting hydrologic deformation using GRACE and GPS, *Geophys. Res. Lett.*, *36*, L15401, doi:10.1029/2009GL038718.
- Trenberth, K., and L. Smith (2005), The mass of the atmosphere: A constraint on global analyses, *J. Clim.*, *18*, 864–875, doi:10.1175/JCLI-3299.1.
- Trenberth, K. E., J. R. Christy, and J. G. Olson (1987), Global atmospheric mass, surface pressure, and water vapor variations, *J. Geophys. Res.*, *92*, 14,815–14,826, doi:10.1029/JD092iD12p14815.

- van Dam, T., J. M. Wahr, and D. Lavalée (2007), A comparison of annual vertical crustal displacements from GPS and Gravity Recovery and Climate Experiment (GRACE) over Europe, *J. Geophys. Res.*, *112*, B03404, doi:10.1029/2006JB004335.
- van Dam, T. M., and T. A. Herring (1994), Detection of atmospheric pressure loading using very long baseline interferometry measurements, *J. Geophys. Res.*, *99*, 4505–4517, doi:10.1029/93JB02758.
- van Dam, T. M., and J. Wahr (1987), Displacements of the Earth's surface due to atmospheric loading: Effects on gravity and baseline measurements, *J. Geophys. Res.*, *92*, 1281–1286, doi:10.1029/JB092iB02p01281.
- van Dam, T. M., G. Blewitt, and M. Heflin (1994), Detection of atmospheric pressure loading using the Global Positioning System, *J. Geophys. Res.*, *99*, 23,939–23,950, doi:10.1029/94JB02122.
- van Dam, T. M., J. Wahr, Y. Chao, and E. Leuliette (1997), Predictions of crustal deformation and geoid and sea level variability caused by oceanic and atmospheric loading, *Geophys. J. Int.*, *129*, 507–517, doi:10.1111/j.1365-246X.1997.tb04490.x.
- Wu, X., M. B. Heflin, E. R. Ivins, D. F. Argus, and F. H. Webb (2003), Large-scale global surface mass variations inferred from GPS measurements of load-induced deformation, *Geophys. Res. Lett.*, *30*(14), 1742, doi:10.1029/2003GL017546.
- Zerbini, S., B. Richter, M. Negusini, C. Romagnoli, D. Simon, F. Domenichini, and W. Schwahn (2001), Height and gravity variations by continuous GPS, gravity and environmental parameter observations in the southern Po Plain, near Bologna, Italy, *Earth Planet. Sci. Lett.*, *192*, 267–279, doi:10.1016/S0012-821X(01)00445-9.
- Zdunkowski, W., and A. Bott (2004), *Thermodynamics of the Atmosphere: A Course in Theoretical Meteorology*, 251 pp., Cambridge University Press, Cambridge, U. K.
- Z. Altamimi and X. Collilieux, Laboratoire de Recherche en Géodésie Institut Géographique National, 6–8 Av. Blaise Pascal, F-77455 Marne-La-Vallée, France.
- J. Ray, National Geodetic Survey, NOAA, N/NGS6, SSMC3/8117, 1315 East–West Hwy., Silver Spring, MD 20910-3282, USA.
- T. van Dam, Faculté des Sciences, de la Technologie et de la Communication, University of Luxembourg 6, rue Richard Coudenhove-Kalergi, L-1359 Luxembourg, Luxembourg. (tonie.vandam@uni.lu)